

Modeling of Stimulated Hydrogel Volume Changes in Photonic Crystal Pb^{2+} Sensing Materials

Alexander V. Goponenko and Sanford A. Asher*

Contribution from the Department of Chemistry, University of Pittsburgh,
Pittsburgh, Pennsylvania 15260

Received March 7, 2005; E-mail: asher@pitt.edu

Abstract: We modeled the stimulated hydrogel volume transitions of a material which binds Pb^{2+} and is used as a photonic crystal chemical sensing material. This material consists of a polymerized crystalline colloidal array (PCCA) hydrogel which contains a crown ether molecular recognition group. The PCCA is a polyacrylamide hydrogel which embeds a crystalline colloidal array (CCA) of monodisperse polystyrene spheres of ~ 100 nm. The array spacing is set to diffract light in the visible spectral region. Changes in the hydrogel volume induced by Pb^{2+} binding alter the array spacing and shift the diffracted wavelength. This system allows us to sensitively follow the hydrogel swelling behavior which results from the immobilization of the Pb^{2+} by the crown ether chelating groups. Binding of the Pb^{2+} immobilizes its counterions. This results in a Donnan potential, which results in an osmotic pressure which swells the hydrogel. We continue here our development of a predictive model for hydrogel swelling based on Flory's theory of gel swelling. We are qualitatively able to model the PCCA swelling but cannot correctly model the large responsivity observed at the lowest Pb^{2+} concentrations which give rise to the experimentally observed low detection limits for Pb^{2+} . These PCCA materials enable stimulated hydrogel volume transitions to be studied.

Introduction

Our laboratory has been developing a series of photonic crystal chemical sensing materials which can be used to optically determine analytes.^{1–5} The photonic crystal material is called a polymerized crystalline colloidal array (PCCA) and consists of a hydrogel which embeds a crystalline colloidal array (CCA) of particles that diffract light in the visible spectral region.^{6,7} The array of particles self-assemble into an fcc lattice. Diffraction from the 111 plane of the CCA lattice is designed to report on the volume of the hydrogel.⁸ A molecular recognition agent is attached to the hydrogel or to the particles. The molecular recognition agent actuates a hydrogel volume change in response to analyte interactions. This changes the lattice spacing, which shifts the diffracted wavelength.

We demonstrated a number of different motifs for sensing analytes. For example, we demonstrated a motif that changes the free energy of mixing of the hydrogel,⁹ motifs that change the hydrogel cross-link density,^{4,10} and motifs that change the number of bound ions.^{1–3,11,12} In addition, for each motif we attempted to model the response in the context of the theory of hydrogel swelling. The earlier stage of this modeling examined the hydrogel volume changes which occur for PCCA with attached carboxyl groups in response to pH changes.¹¹ This work was followed by the development of glucose sensors which responded to changing the covalently attached charge on the hydrogel.¹²

We considered in detail all three components of the model: the free energy of mixing, the free energy of the elastic network, and the free energy of Donnan-type equilibrium. We experimentally determined the hydrogel cross-link density, the hydrogel Flory–Huggins interaction parameter, and the affinity constant and concentration of the molecular recognition groups.

These PCCA chemical sensors enable a more careful examination of hydrogel volume changes since they directly and accurately report the volume as the chemical environment is altered. We can then model these volume changes in the context

- (1) Holtz, J. H.; Asher, S. A. *Nature* **1997**, *389*, 829–832.
- (2) Holtz, J. H.; Holtz, J. S. W.; Munro, C. H.; Asher, S. A. *Anal. Chem.* **1998**, *70*, 780–791.
- (3) Reese, C. E.; Baltusavich, M. E.; Keim, J. P.; Asher, S. A. *Anal. Chem.* **2001**, *73*, 5038–5042. Reese, C. E.; Asher, S. A. *Anal. Chem.* **2003**, *75*, 3915–3918.
- (4) Asher, S. A.; Sharma, A. C.; Goponenko, A. V.; Ward, M. M. *Anal. Chem.* **2003**, *75*, 1676–1683.
- (5) Asher, S. A.; Holtz, J. H. U.S. Patent 5,854,078, 1998. Asher, S. A.; Holtz, J. H. U.S. Patent 5,898,004, 1999.
- (6) Asher, S. A.; Jagannathan, S. U.S. Patent 5,281,370, 1994. Rundquist, P. A.; Photinos, P.; Jagannathan, S.; Asher, S. A. *J. Chem. Phys.* **1989**, *91*, 4932–4941. Asher, S. A.; Weissman, J. M.; Tikhonov, A.; Coalson, R. D.; Kesavamoorthy, R. *Phys. Rev. E* **2004**, *69*, 066619.
- (7) Reese, C. E.; Guerrero, C. D.; Weissman, J. M.; Lee, K.; Asher, S. A. *J. Colloid Interface Sci.* **2000**, *232*, 76–80.
- (8) Krieger, I. M.; O'Neill, F. M. *J. Am. Chem. Soc.* **1968**, *90*, 3114–3120. Hiltner, P. A.; Krieger, I. M. *J. Phys. Chem.* **1969**, *73*, 2386–2389. Carlson, R. J.; Asher, S. A. *Appl. Spectrosc.* **1984**, *38*, 297–304. Flaugh, P. L.; O'Donnell, S. E.; Asher, S. A. *Appl. Spectrosc.* **1984**, *38*, 847–850. Asher, S. A. U.S. Patent 4,627,689, 1986.

- (9) Sharma, A.; Jana, T.; Kesavamoorthy, R.; Shi, L.; Virji, M.; Finegold, D.; Asher, S. A. *J. Am. Chem. Soc.* **2004**, *126*, 2971–2977.
- (10) Alexeev, V. L.; Sharma, A. C.; Goponenko, A. V.; Das, S.; Lednev, I. K.; Wilcox, C. S.; Finegold, D. N.; Asher, S. A. *Anal. Chem.* **2003**, *75*, 2316–2323. Alexeev, V.; Das, S.; Finegold, D. N.; Asher, S. A. *Clin. Chem.* **2004**, *50*, 2353–2360.
- (11) Lee, K.; Asher, S. A. *J. Am. Chem. Soc.* **2000**, *122*, 9534–9537.
- (12) Asher, S. A.; Alexeev, V. L.; Goponenko, A. V.; Sharma, A. C.; Lednev, I. K.; Wilcox, C. S.; Finegold, D. N. *J. Am. Chem. Soc.* **2003**, *125*, 3322–3329.

of defined concentrations of analytes added in situations where we can independently determine the affinity of the molecular recognition agents. As discussed below, we can qualitatively model the hydrogel volume swelling induced by Donnan potential osmotic pressures by using the simple Flory theory of ionic gels.¹³ However, our experimentally determined responses are larger than we can theoretically account for; as a result, our sensors are more sensitive than we can explain, a rare situation. These results clearly indicate that further work is required to understand the response of hydrogels to even the simplest perturbations, such as small changes in the number of bound charges.

Experimental Section

NaCl (JT Baker), NaNO₃ (JT Baker), Pb(NO₃)₂ (MCB), and Pb(C₂H₃O₂)₂·3H₂O (EM Science) were used as received. Purified water (18 MΩ) was obtained from a NANOpure Infinity purification system (Barnstead/ThermoLyne Corp., USA). Highly charged, monodisperse polystyrene colloids were prepared via emulsion polymerization, as described elsewhere.⁷

We fabricated the Pb²⁺-responsive PCCA using methods similar to those of Holtz et al.^{1,2} We polymerized a solution contained 89.8 mg of acrylamide (Fluka), 2.87 mg of *N,N*-methylenebisacrylamide (Fluka), 26.9 mg of 4-acrylamidobenzo-18-crown-6 (AAB18C6, Acros Organics), and 1.79 g of a ~10 wt % dispersion of 106-nm-diameter highly charged, monodisperse polystyrene colloidal particles.⁷ The resulting dispersion diffracted 350-nm light that was incident normal to the fcc 111 plane which oriented parallel to the container walls. Wet ion-exchange resin (Bio-Rad, mixed bed AG501-X8(D)) and 8 drops of a 10% solution of diethoxyacetophenone (Aldrich) in DMSO (Fisher) were added, and the mixture was shaken for 30 min. The mixture was centrifuged to remove bubbles and injected between two quartz plates separated by a Parafilm spacer (125 μm thick). The colloidal particles self-assembled into a CCA to give a diffracting liquid film (diffraction maximum 390 nm for normal incident light). This film was photopolymerized into a PCCA by exposure for 1 h to 365-nm UV light from two mercury lamps (Black Ray).

The polymerizing cell was opened, and the PCCA was washed thoroughly with water. We modified the surface of one of the quartz plates with a Sigmacote hydrophobic coating to aid in the release of the PCCA from one surface. The PCCA adhered strongly to the other quartz plate. Our diffraction measurements were obtained with the PCCA attached to the unmodified quartz plate, except as otherwise noted.

Diffraction spectra were measured by using a USB2000 fiber optic spectrometer and an LS-1 tungsten halogen light source (Ocean Optics Inc., USA). UV/vis spectra were measured by using a Cary 5000 UV–vis–NIR spectrophotometer (Varian Inc., USA).

Results and Discussion

Figure 1 shows the dependence of the PCCA diffraction spectra and the Pb²⁺ concentration dependence of the diffraction wavelength. The PCCA diffraction redshifts with increasing Pb²⁺ concentrations due to the complexation of the Pb²⁺ to the 4-acrylamidobenzo-18-crown-6 crown ether groups.^{1–3} This results in the formation of an ionic gel, in which the bound Pb²⁺ immobilizes its counterions and creates a Donnan equilibrium osmotic pressure for low ionic strength solutions. This osmotic pressure swells the gel and redshifts the diffraction.

The Donnan potential is attenuated in high ionic strength solutions. Thus, the hydrogel swelling is reduced, which

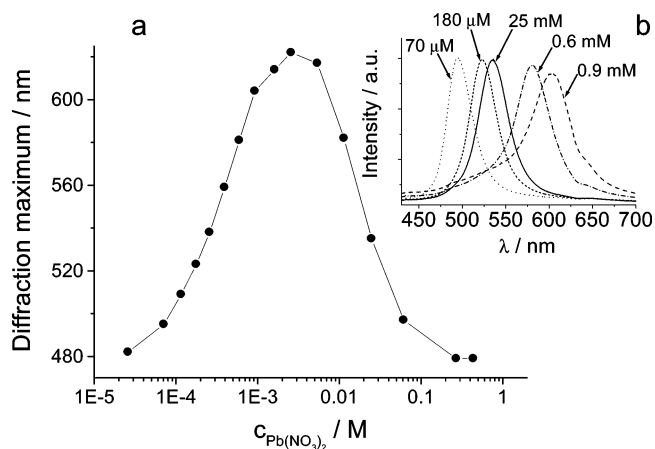


Figure 1. (a) Pb²⁺ concentration dependence of PCCA diffraction. (b) Diffraction spectra of PCCA. The solutions were made by adding a Pb(NO₃)₂ stock solution to pure water. Lines connecting experimental points are to aid the eye.

decreases the responsivity of the PCCA to high concentrations of Pb²⁺.

The response of the PCCA to Pb²⁺ can be understood in the context of hydrogel swelling.¹³ We must first relate the magnitude of the diffraction shift to the hydrogel volume change. For uniform three-dimensional (3-D) swelling, the diffraction maximum will be proportional to the cube root of the hydrogel volume ($\lambda \sim V^{1/3}$). However, if a thin PCCA adheres strongly to one quartz plate, it will only be able to expand in one dimension, along its thickness (1-D swelling); the wavelength of diffraction in this case will be directly proportional to the hydrogel volume ($\lambda \sim V$).

In the general case, to relate the diffraction shift to the hydrogel volume change, one should take into account that the volume of the colloidal particles remains the same during swelling and that the refractive index of the hydrogel changes with PCCA volume changes. We ignored the impact of the colloidal particles since their volume fraction is very small (1–2%). Further, we also ignored the small refractive index shifts of the system which resulted from its composition changes. Our neglect of these issues produces <1% errors.

Further discussion on the difference between 1-D and 3-D swelling of a nonionic hydrogel and how the Flory–Huggins interaction parameter and the cross-link density can be determined from these different swelling behaviors (Appendix 1), an attempt to experimentally measure the response of a PCCA in the regime of 3-D swelling (Appendix 2), and how we determined the concentration of the crown ether molecular recognition groups in the PCCA (Appendix 3) appears in the Supporting Information. Our determination of the affinity constant of the PCCA-bound AAB18C6 crown ether groups was recently described in detail.¹⁴

Hydrogel Swelling in the Absence of Charged Species.

When a PCCA is removed from the polymerization chamber, washed, and equilibrated in pure water, its volume changes until it reaches its *pure water equilibrium volume*. In general our PCCA swells. The total free energy of a nonionic hydrogel at a particular hydrogel volume (G_T) is composed of the free energy of mixing between the hydrogel and the solvent (G_M)

(13) Flory, P. J. *Principles of Polymer Chemistry*; Cornell University Press: Ithaca, NY, 1953.

(14) Geary, C. D.; Zudans, I.; Goponenko, A. V.; Asher, S. A.; Weber, S. G. *Anal. Chem.* **2004**, *77*, 185–192.

plus the free energy associated with the network elasticity (G_E).¹³

$$G_T = G_M + G_E \quad (1)$$

According to Flory–Huggins theory, for a single infinitely long macromolecule, the mixing free energy difference between a polymer solution at a φ volume fraction and an infinitely dilute solution is

$$\Delta G_M = k_B T [n \ln(1 - \varphi) + n\chi\varphi] \quad (2)$$

where k_B , T , n , and χ are the Boltzmann constant, the temperature, the number of solvent molecules in the gel, and the Flory–Huggins interaction parameter, respectively.

The elastic free energy difference is generally modeled by using either the affine or phantom model.^{13,15} For a cross-link functionality of four, the elastic free energy difference between the existing network configuration and the statistically most probable configuration of the network chains is

$$\begin{aligned} \Delta G_E &= \frac{k_B T n_{\text{cr}}}{2} \left[\left(\frac{l^x}{l_m^x} \right)^2 + \left(\frac{l^y}{l_m^y} \right)^2 + \left(\frac{l^z}{l_m^z} \right)^2 - 3 - \ln \left(\frac{l^x l^y l^z}{l_m^x l_m^y l_m^z} \right) \right] \\ &\quad \text{affine model} \\ &= \frac{k_B T n_{\text{cr}}}{4} \left[\left(\frac{l^x}{l_m^x} \right)^2 + \left(\frac{l^y}{l_m^y} \right)^2 + \left(\frac{l^z}{l_m^z} \right)^2 - 3 \right] \\ &\quad \text{phantom model} \quad (3) \end{aligned}$$

where n_{cr} is the effective number of cross-linked chains in the network, l^x , l^y , and l^z are the lengths of the assumed rectangular gel prism in the existing network configuration (oriented along the principal axes of strain), and l_m^x , l_m^y , and l_m^z are the lengths of the rectangular gel prism in the statistically most probable configuration.

We use a critical and enabling assumption, that the hydrogel polymerization occurred under conditions where cross-linked chains occurred in their statistically most probable configurations, such that both the total volume and the shape of the prepared PCCA are identical to those of the statistically most probable configuration.^{11,16} In both cases considered here, 1-D and 3-D swelling, the principal axes of strain are oriented along the length, width, and thickness of the PCCA. Thus, we assume l_m^x , l_m^y , and l_m^z to be identical to the dimensions of the polymerized PCCA, and that l^x , l^y , and l^z are the dimensions of the PCCA under consideration. The volume of the initially prepared PCCA is $V_m = l_m^x l_m^y l_m^z$, while the volume of a shrunken or swollen PCCA is $V = l^x l^y l^z$.

Since the reference states for ΔG_M and for ΔG_E are different, the reference state for a value of ΔG_T (or even where $\Delta G_T = 0$) has no physical meaning. This reference state is also unimportant since we need only the volume derivative of ΔG_T , which gives rise to the osmotic pressure.

Any change in volume upon immersion of the prepared PCCA into an infinite reservoir of pure water is driven by the necessary equalization of the water chemical potentials between the

hydrogel and the surrounding reservoir. The osmotic pressure within the PCCA actuates any volume changes.

At equilibrium, the total osmotic pressure must be zero:

$$\Pi_T = - \frac{\partial \Delta G_T}{\partial V} = \Pi_M + \Pi_E = - \frac{\partial \Delta G_M}{\partial V} - \frac{\partial \Delta G_E}{\partial V} = 0 \quad (4)$$

The hydrogel osmotic pressure which arises from the free energy of mixing of the hydrogel with water is¹¹

$$\Pi_M = - \frac{RT}{V_s} \left[\ln \left(1 - \frac{V_0}{V} \right) + \frac{V_0}{V} + \chi \left(\frac{V_0}{V} \right)^2 \right] \quad (5)$$

where R is the universal gas constant, V_0 is the dry polymer volume, and V_s is the molar volume of the solvent.

The osmotic pressure which results from the network elasticity for uniform 3-D swelling is

$$\begin{aligned} \Pi_E &= - \frac{RT n_{\text{cr}}}{V_m} \left[\left(\frac{V_m}{V} \right)^{1/3} - \frac{1}{2} \frac{V_m}{V} \right] \quad \text{affine model} \\ &= - \frac{RT n_{\text{cr}}}{2 V_m} \left(\frac{V_m}{V} \right)^{1/3} \quad \text{phantom model} \quad (6a) \end{aligned}$$

where n_{cr} is now the effective number of cross-linked chains in the network in moles.

For a hydrogel that can only swell along the z -direction (1-D swelling), $l^x = l_m^x$ and $l^y = l_m^y$ for any volume. The osmotic pressure due to the hydrogel elasticity becomes

$$\begin{aligned} \Pi_E &= - \frac{RT n_{\text{cr}}}{V_m} \left[\frac{V}{V_m} - \frac{1}{2} \frac{V_m}{V} \right] \quad \text{affine model} \\ &= - \frac{RT n_{\text{cr}}}{2 V_m} \frac{V}{V_m} \quad \text{phantom model} \quad (6b) \end{aligned}$$

By substituting eqs 5 and 6b into eq 4, we can determine from the swelling of the gel in pure water the correlation between the Flory–Huggins interaction parameter χ and the effective chain concentration n_{cr}/V_m (see Appendix 1 in the Supporting Information).

Modeling of PCCA Response to Pb^{2+} Concentration. The hydrogel swells and the PCCA diffraction redshifts in the presence of Pb^{2+} due to the immobilization of Pb^{2+} on the polymer network, which results in a difference in the concentrations of mobile nonbound ions inside and outside the gel.¹³ The total osmotic pressure of the resulting ionic network now includes the osmotic pressure Π_{ion} arising from the difference in mobile ions' concentrations inside and outside the hydrogel:

$$\Pi_T = \Pi_M + \Pi_E + \Pi_{\text{ion}} \quad (7)$$

For a dilute solution, Π_{ion} can be approximated by¹³

$$\Pi_{\text{ion}} = RT \sum_x (c_x - c_x^*) \quad (8)$$

where c_x and c_x^* are the concentrations of mobile ions inside and outside the hydrogel. The mobile ion concentration differences dominate Π_{ion} .¹⁷ Even the repulsive interactions between

(15) Erman, B.; Mark, J. E. *Structures and properties of rubberlike networks*; Oxford University Press: New York, 1997.

(16) Peppas, N. A.; Merrill, E. W. *J. Polym. Sci., Polym. Chem. Ed.* **1976**, *14*, 441–457.

(17) Ricka, J.; Tanaka, T. *Macromolecules* **1984**, *17*, 2916–2921.

the colloidal particles are negligible compared to the osmotic pressure which derives from the mobile ion concentration differences.

We examined the utility of previously used approaches to improve the ionic species modeling by utilizing corrections based on the Debye–Hückel limiting law.¹⁸ We examined two limits, where the attached charged groups are fixed and where the network-attached charged groups are considered to be mobile.¹⁷ In agreement with other studies,^{17,19} these corrections did not significantly improve our modeling.

Our modeling includes the dication Pb^{2+} , a single-charged cation such as Na^+ added to the samples, and single-charged counterions (A^-) needed to fulfill the electrostatic neutrality condition, which requires that the sum of all charges inside the hydrogel be zero. The concentration of mobile cations and anions in the gel is

$$c_{\text{A}} = c_{\text{Na}} + 2c_{\text{Pb}} + iC_{\text{p}} \quad (9)$$

where i is the fraction of crown ether groups bound to Pb^{2+} times the charge, $z = +2$, and C_{p} is the concentration of crown ether groups, which will be inversely proportional to the changing hydrogel volume, $C_{\text{p}} = n_{\text{p}}/V$. The concentrations of crown ether groups were independently determined (Appendix 3, Supporting Information). The value of i can be calculated from the crown ether association constant K :

$$K = \frac{[\text{PCCA-B18C6-Pb}^{2+}]}{[\text{PCCA-B18C6}][\text{Pb}^{2+}]} = \frac{[\text{PCCA-B18C6-Pb}^{2+}]}{(C_{\text{p}} - [\text{PCCA-B18C6-Pb}^{2+}])([\text{Pb}^{2+}])} \quad (10)$$

Thus,

$$i = 2 \frac{Kc_{\text{Pb}}}{1 + Kc_{\text{Pb}}} \quad (11)$$

Rather than obtaining the Donnan ratio, $c_{\text{A}}^*/c_{\text{A}}$, from the Donnan potential,¹⁷ we more conveniently determine it by invoking equality of electrolyte activity inside and outside the hydrogel.¹³ Here we approximate the electrolyte activity as the product of the activities of the individual dissociated ions. We obtain

$$c_{\text{Pb}} = \left(\frac{c_{\text{A}}^*}{c_{\text{A}}}\right)^2 c_{\text{Pb}}^* \quad \text{and} \quad c_{\text{Na}} = \frac{c_{\text{A}}^*}{c_{\text{A}}} c_{\text{Na}}^* \quad (12)$$

We utilize eqs 5, 6b, 7, 8, 9, 11, and 12 to calculate the equilibrium gel volume for solutions with various concentrations of $\text{Pb}(\text{NO}_3)_2$ and NaCl .

PCCA Response to $\text{Pb}(\text{NO}_3)_2$ Solutions in Pure Water.

We measured the dependence of diffraction of the crown ether PCCA to different concentrations of $\text{Pb}(\text{NO}_3)_2$ up to 0.4 M. The $\sim 3 \text{ cm} \times 3 \text{ cm} \times 125 \mu\text{m}$ PCCA was exposed to a 50-mL reservoir of pure water. We increased the Pb^{2+} concentration by adding small aliquots of a stock $\text{Pb}(\text{NO}_3)_2$ solution to the reservoir. After a set of measurements, the PCCA was washed

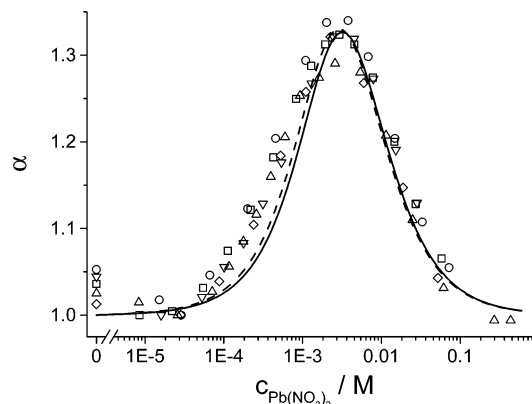


Figure 2. Relative diffraction maximum ($\alpha = \lambda/\lambda_{\text{pure water}}$) of a PCCA as a function of $\text{Pb}(\text{NO}_3)_2$ concentration. Circles, squares, diamonds, and triangles represent different sets of measurements from two PCCA samples. The dashed line was calculated from the affine model, and the solid line was calculated from the phantom model.

thoroughly in pure water and reused later for another set of measurements over a period of four months. This sensor was very stable, showing small changes in diffraction comparable to the inhomogeneity over the sensor surface.

Figure 2 compares the measured diffraction data to our theoretical modeling of the PCCA response to $\text{Pb}(\text{NO}_3)_2$ in pure water. These data derive from five replicate measurements performed on two similar samples. For best comparison between the two independent samples that differed slightly in their initial diffraction maxima, we plotted the data in terms of the relative diffraction maximum, $\alpha = \lambda/\lambda_{\text{pure water}}$, where $\lambda_{\text{pure water}}$ is the diffraction wavelength at equilibrium in pure water.

There is a surprising shrinkage of the PCCA for the lowest Pb^{2+} concentrations up to 20 μM . This behavior is quite different from that observed by Holtz et al.,^{1,2} who observed redshifts for even nanomolar concentrations of Pb^{2+} . We assume that our PCCA contains negatively charged species, such as carboxylates formed by hydrolysis of amides, which cause the PCCA to swell in pure water. We believe that the shrinkage at the lowest Pb^{2+} concentrations results from the increased ionic strengths that occur as the concentration of Pb^{2+} increases.

As we show below, the Donnan equilibrium osmotic pressure for low concentrations of covalently attached charges will be significantly diminished by comparable low concentrations of free electrolytes. In addition, the putative negative covalently attached charge could become neutralized due to binding of Pb^{2+} if ion pairs formed. For our modeling, we assume that our observed minimum diffraction wavelength is that which would have occurred for a neutral PCCA hydrogel in pure water.

Our modeling requires knowing the PCCA crown ether concentration and its association constant. In our modeling, it turns out that errors in one of these values can be offset by compensating errors in the other; an increased crown ether concentration compensates for a lowered affinity.

Thus, we attempted to constrain these values. We used three different independent methods to determine the AAB18C6 solution association constant for Pb^{2+} . We found a surprisingly large range of values from 800 to 2000 M^{-1} . NMR found the highest value, and differential pulse voltammetry found the lowest values. We also measured the association constant of AAB18C6 bound to the gel, K , and found a value of 700 M^{-1} .¹⁴ We chose to use the value $K = 900 \text{ M}^{-1}$ because it is likely be

(18) Bockris, J. O. M.; Reddy, A. K. N. *Modern electrochemistry*, 2nd ed.; Plenum Press: New York, 1998.

(19) English, A. E.; Tanaka, T.; Edelman, E. R. *Polymer* **1998**, *39*, 5893–5897.

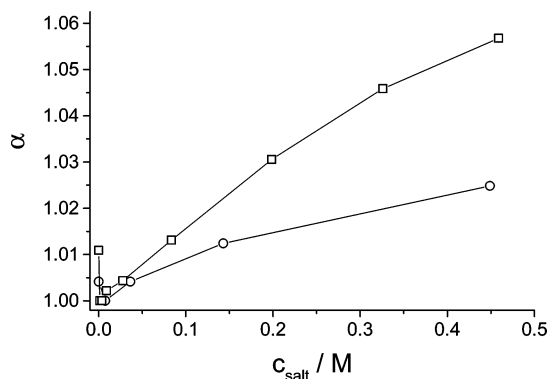


Figure 3. Relative diffraction maximum, α , of PCCA as a function of NaCl (O) and NaNO₃ (□) concentration. Lines connecting experimental points are to aid the eye.

most accurate since it was measured by solution UV absorption spectroscopy. Using this value of K , we found a best fit for AAB18C6l concentration of $n_p/V_m = 5.9$ mM for the affine model and 6.9 mM for the phantom model. In contrast, for $K = 700 \text{ M}^{-1}$, the concentration found is 6.4 and 7.4 mM, respectively. These values are within the error limits of our measured AAB18C6 concentrations (Appendix 3, Supporting Information). We chose to model our data using the phantom model because it appears to be more accurate for hydrogels.¹⁵

Increasing concentrations of Pb(NO₃)₂ result in the formation of an increasingly ionic hydrogel due to complexation of the Pb²⁺. The magnitude of Π_{ion} increases with the increase in the concentration of counterions immobilized within the hydrogel. In addition, as the Pb(NO₃)₂ concentration increases, the ionic strength also increases, which reduces the Donnan potential. This decreases the concentration difference between free ions inside and outside the hydrogel, which decreases the magnitude of Π_{ion} .

This causes the PCCA to initially swell and the diffraction to redshift as the Pb²⁺ concentration increases until the ionic strength increase causes the hydrogel to shrink, which causes the diffraction to then blueshift. We can obtain essentially complete agreement between the model and experimental data for Pb²⁺ concentrations above 1 mM, by slight adjustment of the parameters. However, we find systematic disagreement for the PCCA swelling for Pb²⁺ concentrations below 1 mM; our measured PCCA redshift is larger than we can model.

Dependence of χ on the Solution Composition. PCCA volume changes can also result from changes in the hydrogel χ Flory–Huggins parameter due to solution composition changes. This dependence differs from the Donnan potential hydrogel volume changes, which only depend on the number of ionic species, on their charge, and on the solution ionic strength. We examined the χ -dependent swelling from our PCCA by examining its response to increasing concentrations of salts. Figure 3 shows the dependence of the relative diffraction wavelength maximum of the PCCA on various concentrations of NaCl and NaNO₃. Low concentrations of salt blueshift the diffraction because they reduce the Donnan potential swelling caused by the putative carboxylate ionic impurities in the PCCA. The diffraction then redshifts as the concentration of salt increases. Apparently, the free energy of mixing becomes more favorable as the salt concentration increases.

As shown in Figure 3, twice as big a redshift occurs for NaNO₃ as for NaCl, indicating that the χ parameter depends

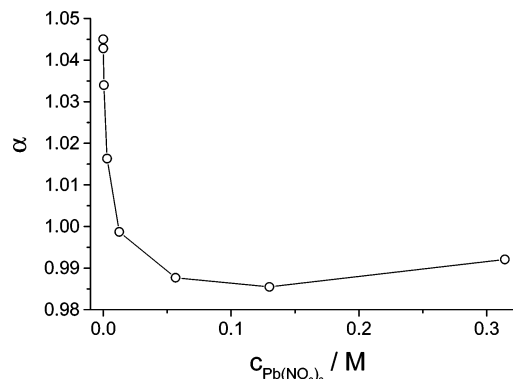


Figure 4. Relative diffraction maximum, α , of PCCA as a function of Pb(NO₃)₂ concentration in a 0.35 M solution of NaNO₃. Lines connecting experimental points are to aid the eye.

on the anion identity. The use of identical cations removes a possible confounding that could occur by binding of Na⁺ to the crown ether groups. Only small diffraction shifts occur for 0.1 M salt concentrations, which indicate that only modest changes in χ occur for the PCCA upon ion concentration changes.

Figure 4 shows the dependence of the diffraction of the PCCA on the Pb(NO₃)₂ concentration in a case where the reservoir contains 0.35 M NaNO₃. These high ionic strengths (>0.1 M salt) dramatically decrease the Donnan potential-induced swelling. Interestingly, increases in the Pb(NO₃)₂ concentration from the lowest concentrations blueshift the diffraction up to 0.1 M. Further increases in the Pb(NO₃)₂ concentration then slightly redshift the diffraction.

Electrostatic effects are unimportant at these high ionic strengths. The blueshift observed at the lowest Pb(NO₃)₂ concentrations must result from the replacement of Na⁺ by Pb²⁺ binding to the AAB18C6. It is possible that the crown ether–Pb²⁺ complex has a less favorable free energy of mixing than the crown ether itself. Alternatively, the larger ionic radius of Pb²⁺ may form bisliganded complexes such as those formed by Cs⁺ which act as cross-links,^{2,4,20} which would blueshift the hydrogel.

Sensor Performance at Different Ionic Strengths. We experimentally and theoretically examined the PCCA response to Pb(NO₃)₂ in solutions containing 1.5, 6.0, and 12 mM NaNO₃, as shown in Figure 5. Figure 6 shows the dependence of the relative diffraction of a 1 mM Pb(NO₃)₂ solution on increasing concentrations of NaNO₃. Both Figures 5 and 6 show excellent agreement of the response at intermediate and high levels of salt, but the theoretical model systematically underestimates the diffraction redshift at lower salt concentrations. At low to intermediate ionic strengths, we underestimate the response of our PCCA to low Pb²⁺ concentrations.

The decreased swelling induced by increasing ionic strength observed here is significantly less than expected on the basis of the behavior of the ionic hydrogels containing carboxylates which were studied previously.¹¹ These acrylamide PCCAs were partially hydrolyzed, and as the pH increased the carboxyl groups titrated and caused the PCCA to increasingly redshift.¹¹ For these pH sensors, 1 mM NaCl solutions decreased the Donnan potential swelling by ~4-fold. In contrast, for the Pb²⁺ sensor, the Donnan potential swelling decreased by only ~10%.

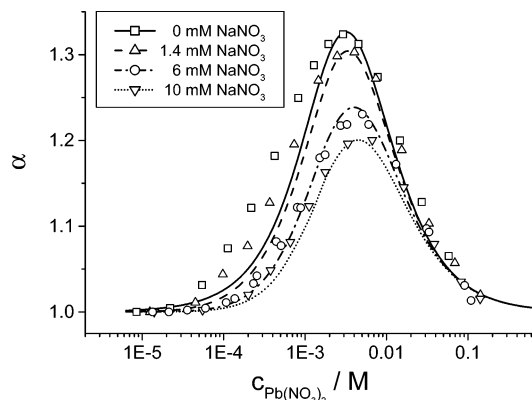


Figure 5. Relative diffraction maximum, α , of PCCA as a function of $\text{Pb}(\text{NO}_3)_2$ concentration in solutions of various concentration NaNO_3 . Circles, squares, and up and down triangles are experimental data. Bold lines were calculated from the phantom model. Affine model results were similar.

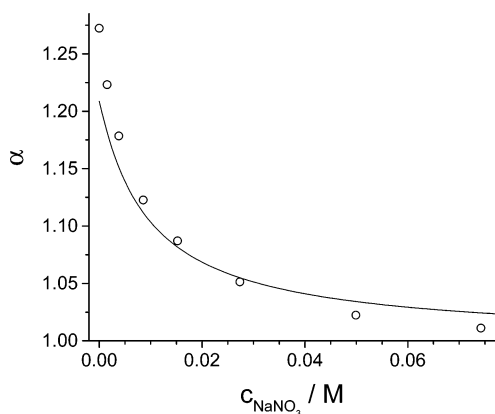


Figure 6. Relative diffraction maximum, α , of PCCA as a function of NaNO_3 concentration for a 1 mM $\text{Pb}(\text{NO}_3)_2$ solution. Circles represent experimental data. The line was calculated from the phantom model. The affine model results were similar.

This difference results from the difference in the concentration of the bound charges. The concentration of the crown ether molecular recognition group in our Pb^{2+} sensor is ~ 5 times larger than the carboxylate concentration in our pH sensors. In addition, the Pb^{2+} charge is twice as big as the OH^- charge. Thus, the Pb^{2+} sensor PCCA hydrogel network is able to bind ~ 10 times more charge. The higher the concentration of bound charges, the higher the ionic strength needed to decrease the Donnan equilibrium osmotic pressure by a particular factor.

Modeling of Ionic Strength Dependence of Osmotic Pressure. If, for example, only single-charged ions are present in solution and the concentration of bound charges is constant, the amount of reduction in the Donnan equilibrium osmotic pressure depends only on the ratio between the electrolyte concentration and the concentration of bound charges; the absolute value of the electrolyte concentration is not relevant. The electrostatic neutrality condition requires that the concentration of mobile cations (c_+) and anions (c_-) inside the hydrogel depends on the average concentration of electrolyte inside the PCCA and on the concentration of bound cation charges c_B , for example:

$$c_+ = c_{\text{el}} - c_B/2 \quad \text{and} \quad c_- = c_{\text{el}} + c_B/2 \quad (13)$$

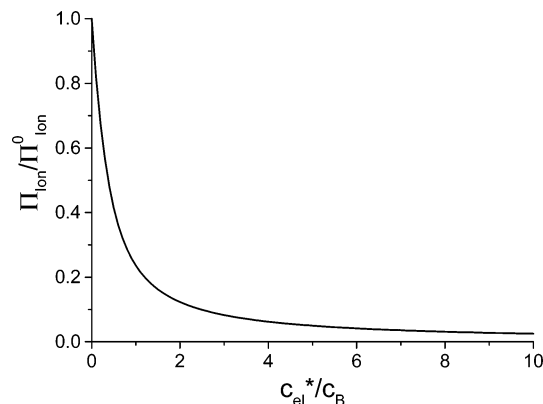


Figure 7. Relative Donnan equilibrium osmotic pressure as a function of the ratio between the electrolyte concentration outside the PCCA and the concentration of bound charges.

The equality of electrolyte activity results in the following relation between electrolyte concentration inside (c_{el}) and outside (c_{el}^*) the PCCA:

$$(c_{\text{el}}^*)^2 = (c_{\text{el}} - c_B/2)(c_{\text{el}} + c_B/2) \quad (14)$$

while the Donnan equilibrium osmotic pressure is proportional to the difference between the electrolyte concentrations:

$$\Pi_{\text{ion}} = 2RT(c_{\text{el}} - c_{\text{el}}^*) \quad (15)$$

Obviously, when the solution outside the PCCA contains no ions, the Donnan equilibrium osmotic pressure (Π_{ion}^0) is related to c_B :

$$\Pi_{\text{ion}}^0 = RTc_B \quad (16)$$

For any other c_{el}^* electrolyte concentration outside the PCCA, eqs 14 and 15 result in

$$\Pi_{\text{ion}} = 2RTc_{\text{el}}^* \left(\sqrt{1 + \frac{1}{4} \left(\frac{c_B}{c_{\text{el}}^*} \right)^2} - 1 \right) \quad (17)$$

Thus, the ratio between the Donnan equilibrium osmotic pressure at a given electrolyte concentration and the Donnan equilibrium osmotic pressure in pure water depends only on the ratio between the electrolyte concentration outside the PCCA and the concentration of bound charges (see Figure 7):

$$\frac{\Pi_{\text{ion}}}{\Pi_{\text{ion}}^0} = 2 \left(\sqrt{\left(\frac{c_{\text{el}}^*}{c_B} \right)^2 + \frac{1}{4}} - \frac{c_{\text{el}}^*}{c_B} \right) \quad (18)$$

This is one of the reasons why the sensitivity of the Pb^{2+} sensor is less affected by the ionic strength than the pH sensor. Another reason is that the presence of Pb^{2+} ions by themselves already results in some ionic strength due to the Pb^{2+} ions and their counterions. To build pH 8, only 10 nM of a base is needed, while 1 mM Pb^{2+} solution contains 2 mM of counterions. If no other salt is added, the Pb^{2+} sensor works at higher ionic strength; adding the same amount of additional salt results in a smaller relative increase of ionic strength for the Pb^{2+} sensor than for the pH sensor.

In these experiments we monitored the PCCA diffraction over a period of four months. Over this period of time, the PCCA,

which was stored in pure water at room temperature, did not show any changes in its response. This demonstrates that the PCCA sensing platform is stable over a long period of time.

These considerations allow us to predict the overall sensor response within a factor of 2 over a wide analyte concentration range in the presence of a wide concentration range of nonassociating electrolytes. We are still unable to model a higher responsivity of our sensors than what we calculate. We will continue to try to improve our models.

Acknowledgment. We gratefully acknowledge financial support from NIH Grant DK55348. We are grateful to Xiangling Xu, who generously supplied us with abundant amounts of colloid.

Supporting Information Available: Appendix 1, describing the difference between 1-D and 3-D swelling of a nonionic hydrogel and how the Flory–Huggins interaction parameter and the cross-link density can be determined from these different swelling behaviors; Appendix 2, describing an attempt to experimentally measure the response of a PCCA in the regime of 3-D swelling; and Appendix 3, describing how we determined the concentration of the crown ether molecular recognition groups in the PCCA. This material is available free of charge via the Internet at <http://pubs.acs.org>.

JA051456P